Solís Oscar (Orcid ID: 0000-0002-8285-5891)
Moratalla Rosario (Orcid ID: 0000-0002-7623-8010)

Optostimulation of striatonigral terminals in substantia nigra induces dyskinesia that increases after L-DOPA in a mouse model of Parkinson's disease

Ettel Keifman[1,2], Irene Ruiz de Diego [1,3], Diego Esteban Pafundo[2], Rodrigo Manuel Paz[2], Oscar Solís[1,3], Mario Gustavo Murer[2*], Rosario Moratalla[1,3*]

1 Instituto Cajal, Consejo Superior de Investigaciones Científicas, CSIC, Avda Dr Arce 37, 28002, Madrid, Spain

2 Universidad de Buenos Aires, CONICET, Instituto de Fisiología y Biofísica (IFIBIO) Bernardo Houssay, Grupo de Neurociencia de Sistemas, Buenos Aires, Argentina

3 CIBERNED, ISCIII, Madrid, Spain

* Equal contribution

Corresponding author:
Prof. Rosario Moratalla
Cajal Institute (CSIC),
Av Dr. Arce 37, 28002 Madrid, Spain.
Tel.: 0034 91 58 54 705; Fax: 0034 91 58 54 754
E-mail address: moratalla@cajal.csic.es

VII. Acknowledgements:

This work was supported by grants from the Spanish Ministries of Economy and Competitiveness (SAF2016-78207-R, PCIN-2015-098) and Health, Social Services and

Equality (PNSD 2016/033, CIBERNED CB06/05/0055) and from the Fundación Ramón Areces (172275, OTR02679). Funding was also provided by the EMHE "Enhancing Mobility between Latin American and Caribbean countries and Europe"-CSIC program, by ANPCYT (Agency for the Promotion of Science and Technology, Argentina), PICT 2013 1523 and 2015 3687 and by the University of Buenos Aires (UBACYT 2018). We thank Jesica Unger and Veronica Risso for their technical assistance.

VIII. Abstract and keywords

ABSTRACT

Background and Purpose:

L-DOPA-induced dyskinesia (LID) remains a major complication of L-DOPA therapy in Parkinson's disease. LID is believed to result from inhibition of substantia nigra reticulata (SNr) neurons by GABAergic striatal projection neurons that become supersensitive to dopamine receptor stimulation after severe nigrostriatal degeneration. Here we asked if stimulation of direct medium spiny neuron (dMSN) GABAergic terminals at the SNr can produce a full dyskinetic state similar to that induced by L-DOPA.

Experimental Approach:

Adult C57BL6 mice were lesioned with 6-hydroxydopamine (6-OHDA) in the medial forebrain bundle. Channelrhodopsin was expressed in striatonigral terminals by ipsilateral striatal injection of adeno-associated viral particles under the CaMKII promoter. Optic fibres were implanted on the ipsilateral SNr. Optical stimulation was performed before and 24 h after three daily doses of L-DOPA at subthreshold and suprathreshold dyskinetic doses. We also examined the combined effect of light stimulation and an acute L-DOPA challenge.

Key Results:

Optostimulation of striatonigral terminals inhibited SNr neurons and induced all dyskinesia subtypes (optostimulation-induced dyskinesia; OID) in 6-OHDA animals, but not in sham-lesioned animals. Additionally, chronic L-DOPA administration sensitized the dyskinetic response to striatonigral terminal optostimulation, as OIDs were more severe 24 h after L-DOPA administration. Furthermore, L-DOPA combined with light stimulation did not result in higher dyskinesia scores than OID alone, suggesting that optostimulation has a masking effect on LID.

Conclusion and Implications:
This work suggests that striatonigral inhibition of basal ganglia output (SNr) is a decisive mechanism mediating LID and identifies the SNr as a target for managing LID.

Keywords: Dyskinesia, L-DOPA, Substantia nigra, D1 receptor, medium spiny neurons, optogenetics.

Abbreviations: 6-OHDA, 6-Hydroxydopamine; AAV, adeno-associated virus; ChR2, channel rhodopsin; D2R, D2 receptor; DA, dopamine; dMSN, direct pathway medium spiny neuron; eYFP, enhanced yellow fluorescent protein; GPi, internal globus pallidus; iMSN, indirect pathway medium spiny neuron; LID, L-DOPA induced dyskinesia; MPTP, 1-methyl-4-phenyl-1,2,3,6-tetrahydropyridine; OID, optogenetically induced dyskinesia; PD, Parkinson's disease; SNr, substantia nigra reticulata; TH, tyrosine hydroxylase.

Ligand/target	Link
Levodopa (L-DOPA)	http://www.guidetopharmacology.org/GRAC/LigandDisplayForward?ligandId=3639
D1 dopamine recetor	http://www.guidetopharmacology.org/GRAC/ObjectDisplayForward?objectId=214&familyId=20&familyType=GPCR
D2 dopamine receptor	http://www.guidetopharmacology.org/GRAC/ObjectDisplayForward?objectId=215&familyId=20&familyType=GPCR
benserazide hydrochloride	http://www.guidetopharmacology.org/GRAC/LigandDisplayForward?ligandId=5150
SCH23390	http://www.guidetopharmacology.org/GRAC/LigandDisplayForward?ligandId=943

	Source	cat #	RRID
DARPP-32	Becton Dickinson	611520	AB_398980
TH	Millipore	152	AB_390204
c-Fos (H-125) antibody	Santa Cruz	sc-7202	AB_2106765
FosB (H-237)	Santa Cruz	Sc- 28213	AB_2106911
C57 ANM	ANM	C57BL/6NCrl	RRID:IMSR_CRL:475
C57/6N Harlan	Harlan barcelona	5825016	RRID:MGI:5825016

INTRODUCTION

L-DOPA-induced dyskinesia (LID) remains a major complication of chronic L-DOPA therapy in Parkinson's disease (PD). LID arises after chronic pulsatile stimulation of striatal dopamine (DA) receptors in patients who, due to severe nigrostriatal terminal degeneration, have lost their capacity to buffer fluctuations of extracellular DA (Cenci et al., 2010; Jenner, 2008; Murer & Moratalla, 2011). However, 1-methyl-4-phenyl-1,2,3,6-tetrahydropyridine (MPTP)-intoxicated patients who quickly develop severe PD symptoms show LID shortly after beginning treatment (Ballard et al., 1985) and similarly a first challenge with L-DOPA induces dyskinesia in severely DA-depleted animals. Furthermore, optogenetic or chemogenetic stimulation of severely dopamine denervated striatal neurons in L-DOPA-naïve rodents can induce dyskinesia resembling LID (Alcacer et al., 2017; F. Hernández et al., 2017; Perez et al., 2017). Altogether this work suggests that loss of DA input can modify striatal circuit function such that striatal activation induces dyskinesia instead of normal actions (Picconi & Calabresi, 2017).

During dyskinesia induced by dopamine receptor stimulation in patients and animal models of PD, neurons at the internal pallidal segment (GPi) and substantia nigra pars reticulata (SNr) are markedly inhibited (Aristieta et al., 2016; Boraud et al., 2001; Filion et al., 1991; Lozano et al., 2000; Meissner et al., 2006; Papa et al., 1999). The main source of SNr inhibition is GABA released by striatal medium spiny neurons of the direct pathway (dMSNs) (Freeze et al., 2013). These neurons express the dopamine D1 receptor (D1R), which is crucial and necessary for the development of LID (Darmopil et al., 2009; Murer & Moratalla, 2011; Halje et al., 2012). Whether the indirect pathway contributes to LID is still controversial. Agonists of D2 receptor (D2R), expressed in the indirect pathway medium spiny neurons (iMSN), only induce dyskinesia in animals that have been primed with mixed D1/D2 agonists (Delfino et al., 2004; Luquin et al., 1992) and do not substantially modify LID in patients (Rascol et al., 2006). Interestingly, LID is not modified by inactivation of D2R (Darmopil et al., 2009), but is reduced by chemogenetic activation of iMSNs (Alcacer et al., 2017). Importantly, in previous studies, stimulation of dMSNs produced dyskinesia that was less intense and varied than that observed with L-DOPA, except when chemogenetic activation of dMSNs was combined with D2 agonist administration. This suggests that D2R inhibition of iMSNs is necessary for full expression of LID (Alcacer et al., 2017) as predicted by classical models and suggest that an activity imbalance between dMSNs and iMSNs drives LID (DeLong, 1990; Jenner, 2008; Suarez et al, 2014, 2016, 2018). However, recent

studies challenge classical views: dMSNs and iMSNs are coactivated during movement (Cui et al., 2013, Parker et al., 2018, (Ryan et al., 2018) and optogenetic co-stimulation of dMSNs and iMSNs induces dyskinesia in PD rats (F. Hernández et al., 2017). Thus, whether selective dMSN stimulation can induce a full repertoire of dyskinetic movements, comparable in intensity to those induced by L-DOPA, remains uncertain.

Here, we asked if optogenetically targeting the densely-packed dMSN terminals at the SNr rather than the broadly distributed dMSN cell bodies at the striatum would generate dyskinetic movements as intense and varied as those produced with L-DOPA. We also asked if dyskinesia-related molecular markers associated with MSN stimulation are expressed during optostimulation of stratonigral axon terminals.

METHODS

Animals

This study was carried out on adult C57BL/6N mice (RRID:MGI:5825016) from Harlan Iberica, Barcelona, Spain. Animals were housed under a 12-hour light/dark cycle with free access to food and water. All experimental procedures conformed to European Community guidelines (2003/65/CE) and were approved by the Cajal Institute's Bioethics Committee (following DC86/609/EU). Electrophysiological experiments performed in Argentina were also carried out in C57BL/6 mice (RRID:IMSR_CRL:475) from the National Academy of Medicine, Buenos Aires, Argentina, following protocols approved by the University of Buenos Aires School of Medicine Institutional Animal Care and Use Committee. Every effort was made to minimise animal discomfort and the overall number of animals used.

Surgical procedures

All surgeries were conducted under deep surgical anaesthesia (1% isoflurane). Animals were mounted on a stereotaxic frame (Kopf Instruments,Tujunga, USA) with a mouse adaptor. 6-Hydroxydopamine (6-OHDA) injection and viral infection were performed during the same surgery. Fibre optic cannulae were implanted in a second surgery 4-6 weeks later.

6-Hydroxydopamine lesion

6-OHDA hydrobromide with added ascorbic acid was dissolved in saline reaching a final concentration of 5.75 µg/µl 6-OHDA in 0.02% ascorbic acid. Mice received 0.7 µl injections of 6-OHDA or vehicle solution into the left medial forebrain bundle at the following

coordinates from bregma (mm): anterior-posterior = -1, medial-lateral = +1.2, dorso-ventral = -4.8. Injections were performed at 0.5 µl/min using a 300 µm-diameter cannula attached to a 1µl Hamilton syringe controlled by a motorised pump (Harvard Apparatus, USA). Special care was required after 6-OHDA lesion to ensure survival. Each mouse was weighed daily and received a subcutaneous injection of saline and an enriched diet. This procedure continued until animals began to regain weight (14-20 days after surgery).

Vector injection

Immediately after 6-OHDA or vehicle infusion, an adeno-associated virus (AAV) vector expressing channelrhodopsin 2 (ChR2) tagged with enhanced yellow fluorescent protein (eYFP) and under the CaMKII promoter (AAV-CaMKIIa-hChR2(H134R)-eYFP) was injected into the left dorsolateral striatum. Viral concentration was 2.46 x 10^{13} viral particles per ml. 0.5 µl AAV was infused in the left striatum at 0.1 µl/min at the following coordinates (mm): anterior-posterior= +0.5, medial-lateral= +2.5 and dorso-ventral= -3. An additional group of 6-OHDA animals was injected with an AAV vector expressing only eYFP (AAV-CaMKIIa-eYFP).

Fibre optic cannula implant

Four to six weeks after 6-OHDA lesion and viral infection, mice were implanted ipsilaterally with a fibre optic cannula over the substantia nigra pars reticulata (SNr). We used the following coordinates (mm): anterior-posterior = -2.9, medial-lateral = +1.4 and dorso-ventral = -4.25. Fibre optic cannulae had a 200µm core fibre, flat cleave and 0.22 NA (Doric Lenses, Quebec, Canada).

Behavioural tests

Three weeks after 6-OHDA injection, behavioural testing was performed on 3 non-consecutive days during the light phase in order to select only severely lesioned animals. All mazes and apparatus were thoroughly cleaned with 10% ethanol and dried between subjects.

Actimeter

General horizontal and vertical exploratory activity in a novel open field was recorded as in Ruiz-DeDiego et al. (2018) using a multi-cage activity meter (Columbus Instruments, Ohio, USA) with 8 individual cages measuring 20 x 20 x 28 cm. Horizontal movement was

detected by 2 arrays of 16 infrared beams, with a third array positioned 4 cm above the floor to detect vertical movement. Test sessions lasted 20 min.

Cylinder test

Each mouse was placed in a 10 cm diameter glass cylinder and videotaped for 3 min. Mice responded to the novel environment by standing on their hindlimbs and leaning on the walls of the cylinder with their forelimbs. The number of supporting ipsilateral, contralateral and simultaneous forepaw placements against the cylinder wall was assessed. Data are expressed as a percentage of contralateral forelimb use (% contralateral forelimb use = (contralateral contacts / (ipsilateral + contralateral + simultaneous contacts / 2) X 100).

Accelerating rotarod test

Mice were tested in sets of five, using an accelerating rotarod (from 4 to 40 rpm in 5 min; Ugo Basile, Rome, Italy). The latency to fall from the rod was automatically recorded and cut-off time was 5 min as in García-Montes et al.(2018). Each animal was assessed in a single day over 6 trials with 15 min inter-trial intervals.

Optical stimulation

Striatonigral terminals were activated using a 473 nm DPSS blue laser (Shanghai Laser, Shanghai, China) with a maximum output power of 100 mW. The laser was controlled by an Optogenetics TTL Pulse Generator (OPTG) (Doric Lenses, Quebec, Canada) and its power was adjusted to be 10 mW at the fibre tip (measured with a PM100D optical power meter with an S120C sensor; Thorlabs Inc, Newton, USA). Two optical stimulation protocols were used in this study. One consisted of a single 15 s pulse, a 3 min pause, and a second single 15s pulse tested at 1-10 mW. The second stimulation protocol consisted of a 30 s burst of pulsed light at 20 Hz with a 5 or 20 ms pulse duration at 10 mW, a 3 min pause and a second 30 s burst of light identical to the first. Only one protocol was tested per session and sessions were separated by at least 72 h. After eliciting dyskinesias with the two light stimulation protocols, animals were subjected to a L-DOPA sensitisation protocol using escalating doses of L-DOPA. L-DOPA methyl ester was injected intraperitoneally once per day, 20 min after an intraperitoneal benserazide hydrochloride injection. L-DOPA and benserazide doses were respectively 2 mg/kg and 6 mg/kg; 3 mg/kg and 6 mg/kg; 6 mg/kg and 6 mg/kg; 9 mg/kg and 12 mg/kg; 20 mg/kg and 12 mg/kg. Animals were light stimulated twice over one week. In the first session, abnormal involuntary movements elicited by laser stimulation were assessed

24 h after three daily doses of L-DOPA. The second session took place 72 h later; the simultaneous effect of light stimulation combined with an acute dose of L-DOPA was assessed. For a graphical explanation of the escalating L-DOPA treatment protocol, please see Figures 4A and 6A.

Dyskinesia ratings

Dyskinesia was rated by two separate raters, one of whom was blind to treatment (sham or lesion), based on video footage. Lineal regression analysis on raters' scores produced an R2=0.84. Therefore, the raters' scores were averaged. Each subtype of dyskinesia (oral, axial, forelimb) was scored, considering dyskinesia frequency and amplitude, as described in (Perez et al., 2017). Briefly, the frequency scale ranged from 0 to 4 (where 0 = no dyskinesia; 1 = occasional dyskinesia displayed for <50% of the observation time; 2 = sustained dyskinesia displayed for >50% of the observation time; 3 = continuous dyskinesia; 4 = continuous dyskinesia not interruptible by external stimuli). Amplitude scores were subdivided as "A," which indicates oral dyskinesia without tongue protrusion, forelimb dyskinesia without shoulder engagement and axial dyskinesia with body twisting <60°, or "B," indicating oral dyskinesia with tongue protrusion, forelimb dyskinesia with shoulder engagement, or axial dyskinesia with body twisting ≥60°. Overall scores for the frequency and amplitude of dyskinesia used for data analysis were calculated as 1A=1, 1B=2, 2A=2, 2B=4, 3A=4, 3B=6, 4A=6, 4B=8. This entails that scores for any one component (axial, oral, or forelimb) may be rated from 0 to 8. Total dyskinesia scores were calculated as the sum of all components, with a total possible maximum score of 24 per rating point.

Tissue preparation

After behavioural testing, animals were illuminated for one final session with the 20Hz 20ms 10mW protocol and perfused 50 minutes later. Mice were anaesthetised (sodium pentobarbital, 100 mg/kg) and perfused transcardially with cold saline containing heparin (500 IU/L) followed by 4% paraformaldehyde (PFA) in phosphate buffer (PB). Brains were then dissected, incubated overnight in PFA and then stored in PB. Fixed brains were cut into 30 µm coronal sections in a vibratome (Leica Microsystems, Wetzlar, Germany) and slices were stored free-floating in 0.1M PB containing 0.1% sodium azide at 4°C until use. 6-OHDA-induced nigrostriatal lesions were confirmed by immunohistochemical detection of tyrosine hydroxylase (TH) on free-floating sections from the striatum (anti-TH 1:1,000; Millipore, Temecula, USA). C-fos, FosB and DARPP-32 expression were assessed by

immunohistochemistry on free-floating striatal sections (anti-c-Fos 1:15,000; anti-FosB 1:7,500; anti-DARPP-32 1:500) as previously described (Ruiz-DeDiego et al., 2015 and Granado et al., 2007).

In vitro electrophysiology

Experiments were conducted in brain slices prepared from the SNr of 6-month-old mice. These mice were sham lesioned and were injected with AAV particles, as described above (*vector injection*), 16 weeks prior to experiments. Mice were deeply anaesthetised with isoflurane and decapitated. Brains were quickly removed and immersed in ice-cold slicing solution containing 210 mM sucrose, 10 mM NaCl, 1.9 mM KCl, 1.2 mM Na_2HPO_4, 33 mM $NaHCO_3$, 6 mM $MgCl_2$, 1 mM $CaCl_2$ and 10 mM glucose; pH 7.3-7.4 when bubbled with 95% O_2 and 5% CO_2. The SNr was then sectioned into 300 µm coronal slices, using a vibrating microtome (Pelco 1000, Ted Pella, Inc). Slices were immediately placed in an incubation chamber filled with artificial cerebrospinal fluid (ACSF) maintained at 36°C and containing 125 mM NaCl, 2.5 mM KCl, 1.25 mM Na_2HPO_4, 10 mM glucose, 25 mM $NaHCO_3$, 0.4 mM ascorbate, 1 mM $MgCl_2$ and 2 mM $CaCl_2$, pH 7.3-7.4 when gassed with 95% O_2 and 5% CO_2. After 5 min incubation at 36°C, brain slices were stabilised at room temperature in the same solution for at least 30 min before they were transferred to the recording chamber.

For recording, slices were transferred to a submersion chamber and superfused at 2 ml. min^{-1} with oxygenated ACSF at 30-32°C. Whole-cell recordings were obtained from visually identified neurons in the SNr using a Nikon microscope equipped with IR-DIC optics. Pipettes pulled from borosilicate glass capillaries had a resistance of 4-6 MΩ when filled with the following solutions. Solution A (used for current clamp experiments): 120 mM potassium gluconate, 10 mM KCl, 10 mM HEPES, 0.2 mM EGTA, 4.5 mM MgATP, 0.3 mM NaGTP, 14 mM sodium phosphocreatine; pH adjusted to 7.2-7.4 with KOH. Solution B (used for voltage clamp experiments): 130 mM $CsMeSO_4$, 10 mM HEPES, 0.2 mM EGTA, 4.5 mM MgATP, 0.3 mM NaGTP, 14 mM sodium phosphocreatine, 10 mM TEA-Cl, 5 mM QX-314-Br; pH adjusted to 7.2-7.4 with CsOH. Recordings were obtained using Multiclamp 700B amplifiers (Molecular Devices, San Jose, USA). Signals were low-pass filtered at 6 kHz and digitised at 20 kHz using DigiData 1200 acquisition interfaces (Molecular Devices). Data acquisition and analysis were performed using Clampex 10.2 and CampFit 10.2 software (Molecular Devices). In voltage-clamp mode, the pipette capacitance was compensated and series resistance was continuously monitored but was not compensated. Only recordings with

a stable series resistance of <20 MΩ were used for analysis. When current-clamp mode was used, series resistance and pipette capacitance were monitored and corrected using bridge and capacitance neutralization.

Data and statistical analysis

Data and statistical analyses comply with the recommendations on experimental design and analysis in pharmacology (Curtis et al., 2015). Data in figures are expressed as mean ± standard error of the mean (SEM). Data omission or exclusion criteria: in some cases, mis-injection of AAV caused insufficient AAV-dependent ChR2 expression, or optic fibres were not placed over the SNr. These animals were excluded, resulting in slightly unbalanced experimental groups. Statistical analysis was performed using SigmaPlot 11.0 (RRID:SCR_003210, Systat Software Inc, UK). The significance level was set at $P < 0.05$. Depending on the number of experimental groups and factors to be compared, statistical analyses were performed with t-tests or two-way or repeated measures ANOVAs followed by post hoc tests (Bonferroni) when appropriate. Before applying parametric tests, data were tested for normality with the Kolmogorov-Smirnov test and homoscedasticity with the Levene median test.

Materials

6-OHDA hydrobromide with added ascorbic acid, L-DOPA, benserazide hydrochloride, NaCl, KCl, Na_2HPO_4, $NaHCO_3$, $MgCl_2$, $CaCl_2$, ascorbate, HEPES, EGTA, MgATP, NaGTP, sodium phosphocreatine, KOH, $CsMeSO_4$, NaGTP, TEA-Cl and CsOH were purchased from Sigma-Aldrich (St. Louis, USA). QX-314-Br was from Tocris (Bristol, UK). AAV was purchased from Vector Core (North Carolina University, Chapel Hill, USA). TH antibody (cat# AB152, RRID: AB_390204) was from Millipore (Burlington, USA). cFos (cat# sc-7202, RRID: AB_2106765) and FosB (cat# Sc- 28213, RRID: AB_2106911) antibodies were from Santa Cruz Biotechnology (Santa Cruz, USA). DARPP-32 antibody (cat# 611520, RRID: AB_398980) was from Becton Dickinson (Franklin Lakes, USA).

Nomenclature of Targets and Ligands aterials

Key protein targets and ligands in this article are hyperlinked to corresponding entries in http://www.guidetopharmacology.org, the common portal for data from the IUPHAR/BPS Guide to PHARMACOLOGY (Harding et al., 2018), and are permanently archived in the Concise Guide to PHARMACOLOGY 2017/18 (Alexander et al., 2017).

RESULTS

Validation of the optogenetic approach in brain slices

To selectively stimulate striatonigral axon terminals in the SNr, we injected adeno-associated viral (AAV) particles expressing the fusion protein ChR2-EYFP, driven by the CaMKIIa promoter, in the striatum of C57BL6 mice. Histology confirmed the expression of ChR2-EYFP in the striatum as well as in the synaptic terminal field of striatonigral neurons in the SNr (Figure 1A). Whole-cell patch clamp recordings of SNr neurons in coronal brainstem slices, 16 weeks after intrastriatal AAV-ChR2-EYFP injection, were used to determine if light stimulation of striatonigral terminals induces GABA-mediated inhibition of SNr neurons (Figure 1B). Exploratory current clamp studies showed that both continuous (1 s) and pulsed train illumination (pulses of 5-20 ms duration at 10-20 Hz; 447 nm light source), at intensities of 1-10 mW, markedly inhibited the firing of SNr neurons (>90% inhibition of firing, 4 cells from two animals, regardless of light stimulation protocol). Voltage clamp studies showed that 1, 5 or 20 ms-long light pulses evoked IPSCs in SNr neurons, which were almost completely blocked by the non-competitive GABA-A receptor antagonist picrotoxin (10 cells from 5 animals; data corresponding to 20 ms pulses are shown in Figure 1C). Additional current clamp experiments were performed to characterize the effect of 20 Hz trains of light pulses, which in preliminary behavioural experiments provided promising results (see below). On average, it was possible to nearly completely inhibit the spontaneous tonic firing of SNr neurons located near the centre of the light field with 20 Hz trains of 5 or 20 ms duration pulses of an intensity of ~8 mW (7 cells from 5 animals; data obtained with 20 ms pulses are shown in Figure 1D-E). Addition of picrotoxin to the bath completely blocked the effect of optostimulation of striatonigral terminals on SNr firing (Figure 1D-E).

These results indicate that ChR2 is efficiently expressed and functional in striatonigral terminals.

Parkinson-like symptoms and dopamine denervation

Parkinson-like phenotypes were tested three weeks after lesion in order to select animals with marked motor coordination deficits (rotarod) and a reduction of contralateral forelimb use (cylinder test) and vertical activity (multicage activity meter system) (Figure 2A-C). Dopaminergic degeneration in these animals was further confirmed post-mortem by immunohistochemistry, assessing TH fibre loss, and determining striatal volume with a

complete loss of TH-immunoreactive fibres (Figure 2D-F). We also verified ChR2-YFP expression in DARPP32-positive striatal neurons and in DARPP32-positive fibres in the SNr – the projection field of dMSNs (Figure 2G).

Optogenetic stimulation of striatonigral terminals induces abnormal involuntary movements in 6-OHDA lesioned mice

To examine the effect of striatonigral terminal optostimulation on dyskinetic behaviour, a fibre optic cannula was implanted on the ipsilateral SNr of lesioned or sham-operated mice transduced with ChR2-EYFP; various light stimulation protocols were tested in sham and 6-OHDA mice. To determine the optimal intensity of light pulses, mice were stimulated with a continuous 15 s blue laser pulse at different intensities (1, 2, 5, 8, 10, 12 mW). Abnormal movements resembling axial, orofacial and limb dyskinesia induced by L-DOPA were readily detected in 6-OHDA-lesioned animals from 2 mW and progressively increased to reach a plateau at 10 mW (Figure 3A). We therefore used 10 mW for subsequent experiments. For pulsatile stimulation, we used 30 s and 10 mW pulse trains at different frequencies (10-20 Hz) and pulse duration (5-20 ms). No dyskinesia was observed with the 10 Hz-5 ms protocol, however, 20 Hz-5 ms elicited weak dyskinetic symptoms (*suboptimal protocol*), which increased at 20 Hz-20 ms bursts (Figure 3B). Dyskinetic symptoms elicited with 20 Hz-20 ms light bursts were similar to those elicited with continuous light. Each pulsatile protocol was tested in two different sessions (48 h apart); each session consisted of two trials, 3 min apart. The scores during intra- and inter-session repetitions of an illumination protocol were similar (Figure 3C). The dyskinesia induced in 6-OHDA-lesioned animals was predominantly of the axial type, but abnormal limb and orofacial movements were also observed (Figure 3D-E). Optostimulation of striatonigral terminals also induced contralateral rotations in 6-OHDA-lesioned mice (Figure 3E-F). In sham-lesioned mice, optostimulation at the SNr with continuous light or with trains of light pulses failed to induce abnormal movements and overall produced very subtle behavioural effects (Figure 3A, B, F). Overall, these data show that in animals with severe nigrostriatal terminal degeneration induced by 6-OHDA, but not in sham-lesioned mice, optostimulation of striatonigral terminals induces a wide repertoire of abnormal movements resembling LID (henceforth termed optostimulation-induced dyskinesia - OID).

Chronic L-DOPA administration sensitises dyskinetic responses to striatonigral terminal optostimulation

Optostimulation of MSN cell bodies induces more dyskinetic movements in L-DOPA-primed than in naïve 6-OHDA-lesioned mice (F. Hernández et al., 2017; Perez et al., 2017; Ryan et al., 2018) . However, it is not known whether this sensitisation depends only on striatal adaptations induced by L-DOPA or if it can be partly accounted for by extrastriatal adaptations. To determine if exposure to L-DOPA sensitises the dyskinetic response to optostimulation of striatonigral terminals, sham and 6-OHDA-lesioned mice were treated with escalating doses of L-DOPA (3, 6, 9, and 20 mg/kg i.p., each dose given for 3 consecutive days) and tested for the effects of optostimulation when they were "off" (L-DOPA-free for 24 h) as represented in the timeline (Figure 4A).

During the course of L-DOPA treatment, there was a significant increase of both OID and LID in the 6-OHDA-lesioned animals. Stimulation (30 s, 20 Hz, 20 ms pulses, 10 mW) of striatonigral terminals consistently induced more dyskinesia in L-DOPA-primed than in naïve 6-OHDA-lesioned mice (Figure 4B). Interestingly, the dyskinesia scores during striatonigral terminals optostimulation were consistently higher than those induced by L-DOPA alone at doses of 3 and 6 mg/kg. However, these differences disappeared when animals received higher doses of L-DOPA. The OID scores measured 24 h after 9 and 20 mg/kg L-DOPA were comparable to those induced by L-DOPA alone (Figure 4B). Sham mice did not show OID at any of the conditions tested (Figure 4B). The significant increase of both the OID and LID scores during L-DOPA treatment indicates a progressive sensitisation to striatonigral terminal optostimulation.

We also asked if OID and LID involve similar repertoires of dyskinetic movements. Indeed, axial dyskinesia prevailed in both conditions, especially at the beginning of treatment. During treatment, for both conditions, limb and orofacial dyskinesia accounted for ~50% of the dyskinetic scores. Overall, orofacial dyskinesia seemed to be less frequent during OID than in LID (Figure 4C).

To rule out any possible contribution of D1-type dopamine receptor stimulation in OID, light stimulation (20 Hz, 20 ms pulses, 10 mW) was applied to striatonigral axon terminals before and 25 min after systemic administration of the prototypical D1-type receptor antagonist SCH23390 (0.2 mg/kg i.p.). As expected, SCH23390 increased time of immobility and reduced vertical activity (Figure 5A-B). However, the D1-type receptor antagonist had no effect on the intensity or composition of OID (Figure 5C-D).

Although our optostimulation protocols were very brief (1 min of light stimulation during each session), the above set of animals was exposed to several illumination sessions before and during L-DOPA treatment. To exclude the possibility that multiple light sessions would generate plastic changes that could interfere with behavioural results, we prepared an additional set of 6-OHDA-lesioned mice (n=4) that received one illumination session before and one 24 h after the last escalating dose of L-DOPA (Figure 6A). In these animals, the OID score was also significantly higher after L-DOPA treatment. Furthermore, there was no difference between the OID score of the last illumination session and the LID score during the last L-DOPA challenge (Figure 6B-C). Importantly, there were no statistical differences in OID between the two sets of animals —main set of animals (figure 4) and additional set of animals (figure 6)— in either naïve or primed conditions.

Finally, to completely rule out any possible non-specific effect of light stimulation in our results, a group of 6-OHDA-lesioned animals was injected in the striatum with an AAV vector carrying eYFP only and subjected to the treatments displayed in figure 6A. Light stimulation of striatonigral axon terminals expressing eYFP (20 Hz, 20ms, 10mW, for 30s) did not induce dyskinesia, neither before, nor after L-DOPA administration (Figure 6B). Importantly, these animals showed strong dyskinesia at 20mg/kg L-DOPA (Figure 6C).

Subthreshold striatonigral terminal optostimulation enhances L-DOPA-induced dyskinesia, but suprathreshold stimulation does not

The above data show that optostimulation of striatonigral terminals induces more dyskinesia in primed than in naïve 6-OHDA mice and that OID can be as diverse and severe as LID. If both treatments were recruiting the same neural substrate, additive/synergistic interactions would be expected at subthreshold doses of the treatments (as shown in previous studies (Alcacer et al., 2017; F. Hernández et al., 2017; Perez et al., 2017). However, if one of the treatments were strong enough to recruit most of the substrate, it would mask the effect of the other treatment. Thus, we next investigated whether there were synergistic or masking interactions between LID and OID.

To test if OID and LID can interact synergistically, 6-OHDA-lesioned mice (n=15) showing almost no dyskinesia with a weak light stimulation protocol (30 s, 20 Hz, 5 ms pulses, 10 mW) were treated with a subthreshold dose of L-DOPA (2 mg/kg). These mice were then tested again for the effect of the illumination protocol 15 min after the L-DOPA challenge (Figure 7A). The combined treatment produced higher dyskinesia scores than either

treatment alone (Figure 7B; $p<0.05$ for the interaction in two-way repeated measures ANOVA), indicating a synergistic effect.

We speculated that if illumination recruited a large part of the striatonigral terminals, and LID depended mainly on the degree of dMSN activation, additional effects of L-DOPA on dMSN cell bodies would not further increase the dyskinesia score. Alternatively, if LID were promoted by pathways parallel to dMSNs, such as D2R-mediated inhibition of the indirect pathway, L-DOPA combined with striatonigral terminals illumination would yield a higher dyskinesia score than illumination alone. The same animals were therefore further tested for the interaction between our standard illumination protocol (30 s, 20 Hz, 20 ms-long pulses, 10 mW) and escalating doses of L-DOPA (3, 6, 9, and 20 mg/kg i.p.) as depicted in Figure 7A.

Importantly, in L-DOPA-primed animals, striatonigral terminal illumination plus L-DOPA did not yield a higher dyskinesia score than illumination alone in any of the conditions tested (Figure 7C). This cannot be attributed to a ceiling effect, since at 3 mg/kg of L-DOPA, the OID and LID scores were well below those at 20 mg/kg L-DOPA. Additionally, the subtypes of dyskinesia composing OID, LID and dyskinesia induced by combined treatment with light and L-DOPA were similar.

Expression of dyskinesia-related molecular markers in the striatum

Increased phosphorylation of ERK1/2 and increased expression of cFos and FosB in dMSNs in the denervated striatum have been directly associated with LIDs (Andersson et al., 1999); Pavón et al., 2006); Darmopil et al., 2009) and also with dyskinesias induced by optogenetic stimulation of striatal cell bodies (Perez et al., 2017; F. Hernandez et al., 2017). We investigated if optostimulation of striatonigral terminals also induces an increase in c-Fos and FosB in the striatum. Nine days after the last L-DOPA administration, sham and 6-OHDA-lesioned animals were stimulated with the same protocol (20Hz 20ms 10 mW, 2 x 30s) and perfused 50 minutes later. We found a slight but significant increase in the expression of c-Fos in the ChR2 striatum of the 6-OHDA-lesion mice compared with the ChR2 striatum of sham mice (Figure 8A). This increase was much smaller than that expected for animals treated with dyskinetic doses L-DOPA and perfused 50 min after the last L-DOPA challenge. For instance, there was a high increase of FosB expression in the 6-OHDA-lesioned mice, which probably reflects residual expression after the last L-DOPA challenge performed nine days before (Figure 8B). FosB expression was observed in approximately 1000 striatal cells/mm^2, which is about 60 to 80% the density of FosB positive cells observed

in the striatum of 6-OHDA-lesioned mice shortly after a dyskinetogenic L-DOPA challenge (Pavon et al., 2006; Darmopil et al. 2009). In contrast, c-Fos was observed in about 50 striatal cells mm^2 (Figure 8A). There were no significant differences in the contralateral striatum or in sham mice.

DISCUSSION

Our results reveal that selective activation of the striatonigral terminals induces dyskinesia in a mouse model of Parkinson's disease, but not in control animals. Importantly, the repertoire of abnormal movements elicited by this optogenetic approach is similar to that induced by L-DOPA. Our study also shows that optical stimulation induces more severe dyskinetic behaviour in L-DOPA-primed mice, indicating that chronic L-DOPA administration sensitises the behavioral response to striatonigral terminals optostimulations. Nevertheless, combination of L-DOPA and optostimulation shows synergy at subthreshold doses of both treatments, yet, suprathreshold light stimulation interferes with the dyskinetic effect of higher L-DOPA doses, suggesting that both treatments act on the same neural substrate (Figure 9). In summary, this work supports that dyskinesia can be triggered by activation of direct pathway axon terminals at the SNr.

Pioneering studies in mice have shown that optogenetic stimulation of dMSN cell bodies (Kravitz et al., 2010) and axon terminals (Borgkvist et al., 2015) cause an increase in normal motor activity and an improvement of Parkinson-like motor symptoms. Improvement of symptoms is linked to inhibition of SNr neurons by GABA released from striatonigral axon terminals (Borgkvist et al., 2015; Freeze et al., 2013), as predicted by classical basal ganglia models (Albin et al., 1989). It is also in line with electrophysiological evidence from studies that find inhibition of GPi and SNr neurons in animal models of PD and patients treated with L-DOPA and mixed D1/D2 agonists (e.g. apomorphine) at doses that reduce parkinsonian symptoms (Boraud et al., 2001; Filion et al., 1991; Lozano et al., 2000; Papa et al., 1999). The latter studies also show that the transition from the "on" therapeutic state to the dyskinetic state is related to an escalation of inhibition at the level of the GPi and SNr (Boraud et al., 2001; Filion et al., 1991; Lozano et al., 2000; Papa et al., 1999). Consistent with the view that LID is mediated by dMSN inhibition of basal ganglia output, optogenetic stimulation of dMSN axon terminals at the level of the SNr induces a full repertoire of dyskinetic movements in PD mice. These movements are as severe as those induced by a high dose of L-DOPA, and even mask LID when both treatments are given simultaneously.

Studies in 6-OHDA-lesioned rodents not previously treated with L-DOPA have shown that optogenetic stimulation of striatal neuron cell bodies can induce abnormal movements (F. Hernández et al., 2017; Perez et al., 2017; Ryan et al.2018). The striatum shows a number of changes after chronic nigrostriatal lesion, including an increase in dMSN somatic excitability (Fieblinger et al., 2014, Suárez et al., 2014, 2016, 2018). Because MSNs fire more spikes in PD animals than controls when depolarizing current is applied through a somatic recording micropipette, a comparable increase in their firing response would be expected if current were instead applied through somatic ChR2 channels. Therefore, changes in MSN somatodendritic excitability could have contributed to dyskinesia induced by optogenetic stimulation in previous studies. Because stimulation of ChR2 at striatonigral axon terminals could have produced antidromic spike invasion of dMSN cell bodies in our experiments, a contribution of changes in dMSN somatodendritic excitability to our results cannot be ruled out. On the other hand, modification of orthodromic activity by local plasticity at or downstream striatonigral axon terminals has very likely contributed to our findings. Borgkvist et al. (2015) have shown that an increased probability of GABA release from striatonigral terminals contributes to a sensitised motor response in 6-OHDA mice. Additionally, a recent study performed in PD patients suggests that inhibitory transmission in the SNr can suffer potentiation after repeated stimulation (Milosevic et al., 2018). Further examples of plasticity mechanisms induced by 6-OHDA lesion in rodents, that could have contributed to OID in our studies, include a reorganisation of functional movement representation maps in the motor cortex (Brown et al., 2004; Viaro et al., 2011) and accompanying structural and functional changes occurring in cortical neurons (Lindenbach & Bishop, 2013; Villalba et al., 2015).

As with dyskinesia induced by optostimulation of striatal cell bodies (F. Hernández et al., 2017; Perez et al., 2017; Ryan et al., 2018), or chemogenetic stimulation of dMSNs (Alcacer et al., 2017), dyskinesia induced by stimulation of striatonigral axon terminals is enhanced after treating 6-OHDA animals with L-DOPA. Interestingly, many of the cellular and circuit adaptations occurring in PD seem to be homeostatic in nature and are partially reversed by L-DOPA therapy (Fieblinger et al., 2014; Suarez et al., 2016, 2018). For instance, L-DOPA treatment does not exacerbate, but instead partially normalizes the somatic excitability of MSNs in 6-OHDA mice (Fieblinger et al., 2014; Suárez et al., 2014, 2016, 2018). Whether the excitability of striatonigral axon terminals is re-established or exacerbated after L-DOPA priming remains unknown, although L-DOPA administration

induces more GABA release in the SNr of L-DOPA-treated than in naïve 6-OHDA animals (Yamamoto et al., 2006). Further adaptations in movement representations in the motor cortex are seen in L-DOPA-treated 6-OHDA animals, which could also contribute to the abnormal response to striatonigral axon terminals stimulation in our experiments (Viaro et al., 2011).

In previous studies, dyskinesia induced by opto- and chemogenetic stimulation of dMSNs was less severe than LID and interacted additively with LID (Alcacer et al., 2017; Perez et al., 2017). These findings were interpreted as supporting that mechanisms beyond dMSN activation contribute to LID. For instance, Alcacer et al. (2017) found dyskinesia scores resembling those observed in LID when chemogenetic activation of dMSN was combined with a D2 agonist, suggesting that D2R inhibition of iMSN is necessary for full expression of LID. Furthermore, a genetic model allowing to "trap" active neurons during LID recruited mainly dMSN but also iMSN (Girasole et al., 2018) and recent studies show modulations of activity in both dMSN and iMSN during LID (Parker et al., 2018; Ryan et al., 2018). However, optostimulation of striatonigral axon terminals can cause more powerful dyskinesia than moderate and even high doses of L-DOPA, which cannot be further increased by combining optostimulation with L-DOPA. Thus, based on our findings, it is not necessary to invoke mechanisms other than striatonigral inhibition of SNr neurons for full expression of LID. It seems likely that targeting striatonigral axon terminals rather than striatal cell bodies can recruit a wider population of dMSNs than in previous optogenetic studies. It is also likely that optogenetic stimulation of axon terminals might allow a more powerful effect on striatonigral outflow than chemogenetic stimulation of dMSNs. Finally, targeting striatonigral axon terminals could provide a more certain means of selectively activating dMSNs, because even when D1R promoters are used to drive the expression of opto/chemogenetic transgenes in striatal neurons, striatal illumination and systemic administration of CNO could affect D1R-expressing striatal neurons other than dMSNs and targets of dMSNs other than the SNr.

Regarding the expression of dyskinesia-related molecular markers, our results show that c-Fos expression is slightly yet significantly higher only in the 6-OHDA-lesioned hemisphere after ChR2 activation in the ipsilateral striatonigral terminals. This result is likely linked to the dyskinetic activity displayed by the animals just 50 minutes before perfusion. FosB expression was also significantly higher in the 6-OHDA lesioned hemisphere, but probably as a consequence of the chronic L-DOPA treatment stopped nine days before perfusion (Andersson et al., 1999; Pavon et al., 2006). Interestingly, this residual population

of FosB positive cells was much higher than the population of cells expressing c-Fos, suggesting that the full dyskinetic state induced by optostimulation of striatonigral terminals produces very limited transcriptional activity in the striatum. In contrast, dyskinesia induced by light stimulation of striatal cell bodies was accompanied by a marked increase in the expression of dyskinesia-related molecular markers (Perez et al., 2017; Hernandez et al., 2017). Whether the observed increase of c-Fos relates to antidromic activity in dMSN or to the dyskinetic motor activity induced before perfusion remains to be determined. Importantly, sham animals, which showed only a slight increase in motor activity during light stimulation, did not show higher c-Fos expression in the ChR2 hemisphere. Together with previous studies showing limited effects of backpropagating action potentials in dMSN dendrites (Day et al., 2008), and studies showing plasticity at inhibitory synapses in the SNr both in animal PD models and patients (Yamamoto et al., 2006; Borgkvist et al., 2015; Milosevic et al., 2018), the data favour the view that local plasticity at striatonigral synapses play a role in our findings.

In conclusion, we show that optostimulation of striatonigral axons can produce a full dyskinetic state in chronically and severely DA-depleted animals that cannot be further modulated by simultaneous administration of L-DOPA. This introduces the striatonigral synapse as a particularly attractive target for future strategies aimed at improving or managing LID in patients.

AUTHOR CONTRIBUTIONS

EK performed all experiments, carried out data quantification and analysis, prepared figures and contributed to the first draft. IRDD and OS carried out data quantification and contributed in optogenetic behavioural testing, figure preparation and the first draft. DEP and RMP performed electrophysiological experiments and reviewed the manuscript. GM and RM conceived the study, provided experimental design, data analysis, procured funding and interpretation of the results and the final version of the manuscript.

COMPETING INTERESTS

The authors declare no competing interests. The authors report no biomedical or financial interests or potential conflicts of interest.

DECLARATION OF TRANPARENCY AND SCIENTIFIC RIGOUR

This Declaration acknowledges that this paper adheres to the principles for transparent reporting and scientific rigour of preclinical research as stated in the BJP guidelines for Design & Analysis, Immunoblotting and Immunochemistry, and Animal Experimentation, and as recommended by funding agencies, publishers and other organisations engaged with supporting research.

References

Albin, R. L., Young, A. B., & Penney, J. B. (1989). The functional anatomy of basal ganglia disorders. *Trends in Neurosciences*, *12*(10), 366–375.

Alcacer, C., Andreoli, L., Sebastianutto, I., Jakobsson, J., Fieblinger, T., & Cenci, M. A. (2017). Chemogenetic stimulation of striatal projection neurons modulates responses to Parkinson's disease therapy. *Journal of Clinical Investigation*, *127*(2), 720–734. https://doi.org/10.1172/JCI90132

Alexander, S. P. H., Christopoulos, A., Davenport, A. P., Kelly, E., Marrion, N. V, Peters, J. A., … Collaborators, C. (2017). THE CONCISE GUIDE TO PHARMACOLOGY 2017/18: G protein-coupled receptors. *British Journal of Pharmacology*, *174*(S1), S17–S129. https://doi.org/10.1111/bph.13878

Andersson, M., Hilbertson, A., & Cenci, M. A. (1999). Striatal fosB Expression Is Causally Linked with l-DOPA-Induced Abnormal Involuntary Movements and the Associated Upregulation of Striatal Prodynorphin mRNA in a Rat Model of Parkinson's Disease. *Neurobiology of Disease*, *6*(6), 461–474. https://doi.org/https://doi.org/10.1006/nbdi.1999.0259

Aristieta, A., Ruiz-Ortega, J. A., Miguelez, C., Morera-Herreras, T., & Ugedo, L. (2016). Chronic L-DOPA administration increases the firing rate but does not reverse enhanced slow frequency oscillatory activity and synchronization in substantia nigra pars reticulata neurons from 6-hydroxydopamine-lesioned rats. *Neurobiology of Disease*, *89*, 88–100. https://doi.org/10.1016/j.nbd.2016.02.003

Ballard, P. A., Tetrud, J. W., & Langston, J. W. (1985). Permanent human parkinsonism due to 1-methyl-4-phenyl-1,2,3,6-tetrahydropyridine (MPTP): seven cases. *Neurology*, *35*(7), 949–956.

Boraud, T., Bezard, E., Bioulac, B., & Gross, C. E. (2001). Dopamine agonist-induced dyskinesias are correlated to both firing pattern and frequency alterations of pallidal neurones in the MPTP-treated monkey. *Brain : A Journal of Neurology*, *124*(Pt 3), 546–

557.

Borgkvist, A., Avegno, E. M., Wong, M. Y., Kheirbek, M. A., Sonders, M. S., Hen, R., & Sulzer, D. (2015). Loss of Striatonigral GABAergic Presynaptic Inhibition Enables Motor Sensitization in Parkinsonian Mice. *Neuron*, *87*(5), 976–988. https://doi.org/10.1016/j.neuron.2015.08.022

Brown, A. R., Hu, B., Antle, M. C., & Teskey, G. C. (2009). Neocortical movement representations are reduced and reorganized following bilateral intrastriatal 6-hydroxydopamine infusion and dopamine type-2 receptor antagonism. *Experimental Neurology*, *220*(1), 162–170. https://doi.org/10.1016/j.expneurol.2009.08.015

Cenci, M. A., & Konradi, C. (2010). Maladaptive striatal plasticity in L-DOPA-induced dyskinesia. *Progress in Brain Research*, *183*, 209–233. https://doi.org/10.1016/S0079-6123(10)83011-0

Cui, G., Jun, S. B., Jin, X., Pham, M. D., Vogel, S. S., Lovinger, D. M., & Costa, R. M. (2013). Concurrent activation of striatal direct and indirect pathways during action initiation. *Nature*, *494*(7436), 238–242. https://doi.org/10.1038/nature11846

Darmopil, S., Martín, A. B., De Diego, I. R., Ares, S., & Moratalla, R. (2009). Genetic Inactivation of Dopamine D1 but Not D2 Receptors Inhibits L-DOPA–Induced Dyskinesia and Histone Activation. *Biological Psychiatry*, *66*(6), 603–613. https://doi.org/10.1016/J.BIOPSYCH.2009.04.025

Day, M., Wokosin, D., Plotkin, J. L., Tian, X., & Surmeier, D. J. (2008). Differential Excitability and Modulation of Striatal Medium Spiny Neuron Dendrites. *The Journal of Neuroscience*, *28*(45), 11603 LP-11614. https://doi.org/10.1523/JNEUROSCI.1840-08.2008

Delfino, M. A., Stefano, A. V, Ferrario, J. E., Taravini, I. R. E., Murer, M. G., & Gershanik, O. S. (2004). Behavioral sensitization to different dopamine agonists in a parkinsonian rodent model of drug-induced dyskinesias. *Behavioural Brain Research*, *152*(2), 297–306. https://doi.org/10.1016/j.bbr.2003.10.009

DeLong, M. R. (1990). Primate models of movement disorders of basal ganglia origin. *Trends in Neurosciences*, *13*(7), 281–285.

F. Hernández, L., Castela, I., Ruiz-DeDiego, I., Obeso, J. A., & Moratalla, R. (2017). Striatal activation by optogenetics induces dyskinesias in the 6-hydroxydopamine rat model of Parkinson disease. *Movement Disorders*, *32*(4), 530–537. https://doi.org/10.1002/mds.26947

Fieblinger, T., Graves, S. M., Sebel, L. E., Alcacer, C., Plotkin, J. L., Gertler, T. S., …

Surmeier, D. J. (2014). Cell type-specific plasticity of striatal projection neurons in parkinsonism and L-DOPA-induced dyskinesia. *Nature Communications*, *5*, 5316. https://doi.org/10.1038/ncomms6316

Filion, M., Tremblay, L., & Bédard, P. J. (1991). Effects of dopamine agonists on the spontaneous activity of globus pallidus neurons in monkeys with MPTP-induced parkinsonism. *Brain Research*, *547*(1), 152–161.

Freeze, B. S., Kravitz, A. V, Hammack, N., Berke, J. D., & Kreitzer, A. C. (2013). Control of basal ganglia output by direct and indirect pathway projection neurons. *The Journal of Neuroscience : The Official Journal of the Society for Neuroscience*, *33*(47), 18531–18539. https://doi.org/10.1523/JNEUROSCI.1278-13.2013

García-Montes, J.-R., Solís, O., Enríquez-Traba, J., Ruiz-DeDiego, I., Drucker-Colín, R., & Moratalla, R. (2018). Genetic Knockdown of mGluR5 in Striatal D1R-Containing Neurons Attenuates l-DOPA-Induced Dyskinesia in Aphakia Mice. *Molecular Neurobiology*. https://doi.org/10.1007/s12035-018-1356-6

Girasole, A. E., Lum, M. Y., Nathaniel, D., Bair-Marshall, C. J., Guenthner, C. J., Luo, L., … Nelson, A. B. (2018). A Subpopulation of Striatal Neurons Mediates Levodopa-Induced Dyskinesia. *Neuron*. https://doi.org/10.1016/j.neuron.2018.01.017

Granado, N., Escobedo, I., O'Shea, E., Colado, M. I., & Moratalla, R. (2007). Early loss of dopaminergic terminals in striosomes after MDMA administration to mice. *Synapse*, *62*(1), 80–84. https://doi.org/10.1002/syn.20466

Halje, P., Tamtè, M., Richter, U., Mohammed, M., Cenci, M. A., & Petersson, P. (2012). Levodopa-Induced Dyskinesia Is Strongly Associated with Resonant Cortical Oscillations. *The Journal of Neuroscience*, *32*(47), 16541 LP-16551. Retrieved from http://www.jneurosci.org/content/32/47/16541.abstract

Jenner, P. (2008). Molecular mechanisms of L-DOPA-induced dyskinesia. *Nature Reviews. Neuroscience*, *9*(9), 665–677. https://doi.org/10.1038/nrn2471

Kravitz, A. V, Freeze, B. S., Parker, P. R. L., Kay, K., Thwin, M. T., Deisseroth, K., & Kreitzer, A. C. (2010). Regulation of parkinsonian motor behaviours by optogenetic control of basal ganglia circuitry. *Nature*, *466*(7306), 622–626. https://doi.org/10.1038/nature09159

Lindenbach, D., & Bishop, C. (2013). Critical involvement of the motor cortex in the pathophysiology and treatment of Parkinson's disease. *Neuroscience & Biobehavioral Reviews*, *37*(10, Part 2), 2737–2750. https://doi.org/https://doi.org/10.1016/j.neubiorev.2013.09.008

Lozano, A. M., Lang, A. E., Levy, R., Hutchison, W., & Dostrovsky, J. (2000). Neuronal recordings in Parkinson's disease patients with dyskinesias induced by apomorphine. *Annals of Neurology*, *47*(4 Suppl 1), S141-6.

Luquin, M. R., Laguna, J., & Obeso, J. A. (1992). Selective D2 receptor stimulation induces dyskinesia in parkinsonian monkeys. *Annals of Neurology*, *31*(5), 551–554. https://doi.org/10.1002/ana.410310514

Meissner, W., Ravenscroft, P., Reese, R., Harnack, D., Morgenstern, R., Kupsch, A., … Boraud, T. (2006). Increased slow oscillatory activity in substantia nigra pars reticulata triggers abnormal involuntary movements in the 6-OHDA-lesioned rat in the presence of excessive extracelullar striatal dopamine. *Neurobiology of Disease*, *22*(3), 586–598. https://doi.org/10.1016/j.nbd.2006.01.009

Metz, G. A., Piecharka, D. M., Kleim, J. A., & Whishaw, I. Q. (2004). Preserved ipsilateral-to-lesion motor map organization in the unilateral 6-OHDA-treated rat model of Parkinson's disease. *Brain Research*, *1026*(1), 126–135. https://doi.org/10.1016/j.brainres.2004.08.025

Milosevic, L., Kalia, S. K., Hodaie, M., Lozano, A. M., Fasano, A., Popovic, M. R., & Hutchison, W. D. (2018). Neuronal inhibition and synaptic plasticity of basal ganglia neurons in Parkinson's disease. *Brain*, *141*(1), 177–190. Retrieved from http://dx.doi.org/10.1093/brain/awx296

Murer, M. G., & Moratalla, R. (2011). Striatal Signaling in L-DOPA-Induced Dyskinesia: Common Mechanisms with Drug Abuse and Long Term Memory Involving D1 Dopamine Receptor Stimulation. *Frontiers in Neuroanatomy*, *5*, 51. https://doi.org/10.3389/fnana.2011.00051

NC-IUPHAR, Pawson, A. J., Southan, C., Faccenda, E., Sharman, J. L., Harding, S. D., … Fabbro, D. (2017). The IUPHAR/BPS Guide to PHARMACOLOGY in 2018: updates and expansion to encompass the new guide to IMMUNOPHARMACOLOGY. *Nucleic Acids Research*, *46*(D1), D1091–D1106. https://doi.org/10.1093/nar/gkx1121

Papa, S. M., Desimone, R., Fiorani, M., & Oldfield, E. H. (1999). Internal globus pallidus discharge is nearly suppressed during levodopa-induced dyskinesias. *Annals of Neurology*, *46*(5), 732–738.

Parker, J. G., Marshall, J. D., Ahanonu, B., Wu, Y. W., Kim, T. H., Grewe, B. F., … Schnitzer, M. J. (2018). *Diametric neural ensemble dynamics in parkinsonian and dyskinetic states*. *Nature* (Vol. 557). https://doi.org/10.1038/s41586-018-0090-6

Pavón, N., Martín, A. B., Mendialdua, A., & Moratalla, R. (2006). ERK Phosphorylation and

FosB Expression Are Associated with L-DOPA-Induced Dyskinesia in Hemiparkinsonian Mice. *Biological Psychiatry*, *59*(1), 64–74. https://doi.org/10.1016/j.biopsych.2005.05.044

Perez, X. A., Zhang, D., Bordia, T., & Quik, M. (2017). Striatal D1 medium spiny neuron activation induces dyskinesias in parkinsonian mice. *Movement Disorders*, *32*(4), 538–548. https://doi.org/10.1002/mds.26955

Picconi, B., & Calabresi, P. (2017). Switching on the lights of dyskinesia: Perspectives and limits of the optogenetic approaches. *Movement Disorders*, *32*(4), 485–486. https://doi.org/10.1002/mds.26999

Rascol, O., Brooks, D. J., Korczyn, A. D., De Deyn, P. P., Clarke, C. E., Lang, A. E., & Abdalla, M. (2006). Development of dyskinesias in a 5-year trial of ropinirole and L-dopa. *Movement Disorders : Official Journal of the Movement Disorder Society*, *21*(11), 1844–1850. https://doi.org/10.1002/mds.20988

Ruiz-DeDiego, I., Fasano, S., Solís, O., Garcia-Montes, J.-R., Brea, J., Loza, M. I., … Moratalla, R. (2018). Genetic enhancement of Ras-ERK pathway does not aggravate L-DOPA-induced dyskinesia in mice but prevents the decrease induced by lovastatin. *Scientific Reports*, *8*(1), 15381. https://doi.org/10.1038/s41598-018-33713-3

Ruiz-DeDiego, I., Mellstrom, B., Vallejo, M., Naranjo, J. R., & Moratalla, R. (2015). Activation of DREAM (Downstream Regulatory Element Antagonistic Modulator), a Calcium-Binding Protein, Reduces L-DOPA-Induced Dyskinesias in Mice. *Biological Psychiatry*, *77*(2), 95–105. https://doi.org/10.1016/J.BIOPSYCH.2014.03.023

Ryan, M. B., Bair-Marshall, C., & Nelson, A. B. (2018). Aberrant Striatal Activity in Parkinsonism and Levodopa-Induced Dyskinesia. *Cell Reports*, *23*(12), 3438–3446.e5. https://doi.org/https://doi.org/10.1016/j.celrep.2018.05.059

Suarez, L. M., Alberquilla, S., García-Montes, J. R., & Moratalla, R. (2018). Differential Synaptic Remodeling by Dopamine in Direct and Indirect Striatal Projection Neurons in Pitx3^{−/−} Mice, a Genetic Model of Parkinson's Disease. *The Journal of Neuroscience*, *38*(15), 3619 LP-3630. Retrieved from http://www.jneurosci.org/content/38/15/3619.abstract

Suarez, L. M., Solis, O., Aguado, C., Lujan, R., & Moratalla, R. (2016). L-DOPA Oppositely Regulates Synaptic Strength and Spine Morphology in D1 and D2 Striatal Projection Neurons in Dyskinesia. *Cerebral Cortex*, *26*(11), 4253–4264. Retrieved from http://dx.doi.org/10.1093/cercor/bhw263

Suárez, L. M., Solís, O., Caramés, J. M., Taravini, I. R., Solís, J. M., Murer, M. G., &

Moratalla, R. (2014). L-DOPA treatment selectively restores spine density in dopamine receptor D2-expressing projection neurons in dyskinetic mice. *Biological Psychiatry*, *75*(9), 711–722. https://doi.org/10.1016/j.biopsych.2013.05.006

Viaro, R., Morari, M., & Franchi, G. (2011). Progressive Motor Cortex Functional Reorganization Following 6-Hydroxydopamine Lesioning in Rats. *Journal of Neuroscience*, *31*(12), 4544–4554. https://doi.org/10.1523/JNEUROSCI.5394-10.2011

Villalba, R. M., Mathai, A., & Smith, Y. (2015). Morphological changes of glutamatergic synapses in animal models of Parkinson's disease. *Frontiers in Neuroanatomy*, *9*, 117. https://doi.org/10.3389/fnana.2015.00117

Yamamoto, N., Pierce, R. C., & Soghomonian, J.-J. (2006). Subchronic administration of l-DOPA to adult rats with a unilateral 6-hydroxydopamine lesion of dopamine neurons results in a sensitization of enhanced GABA release in the substantia nigra, pars reticulata. *Brain Research*, *1123*(1), 196–200. https://doi.org/10.1016/j.brainres.2006.09.027

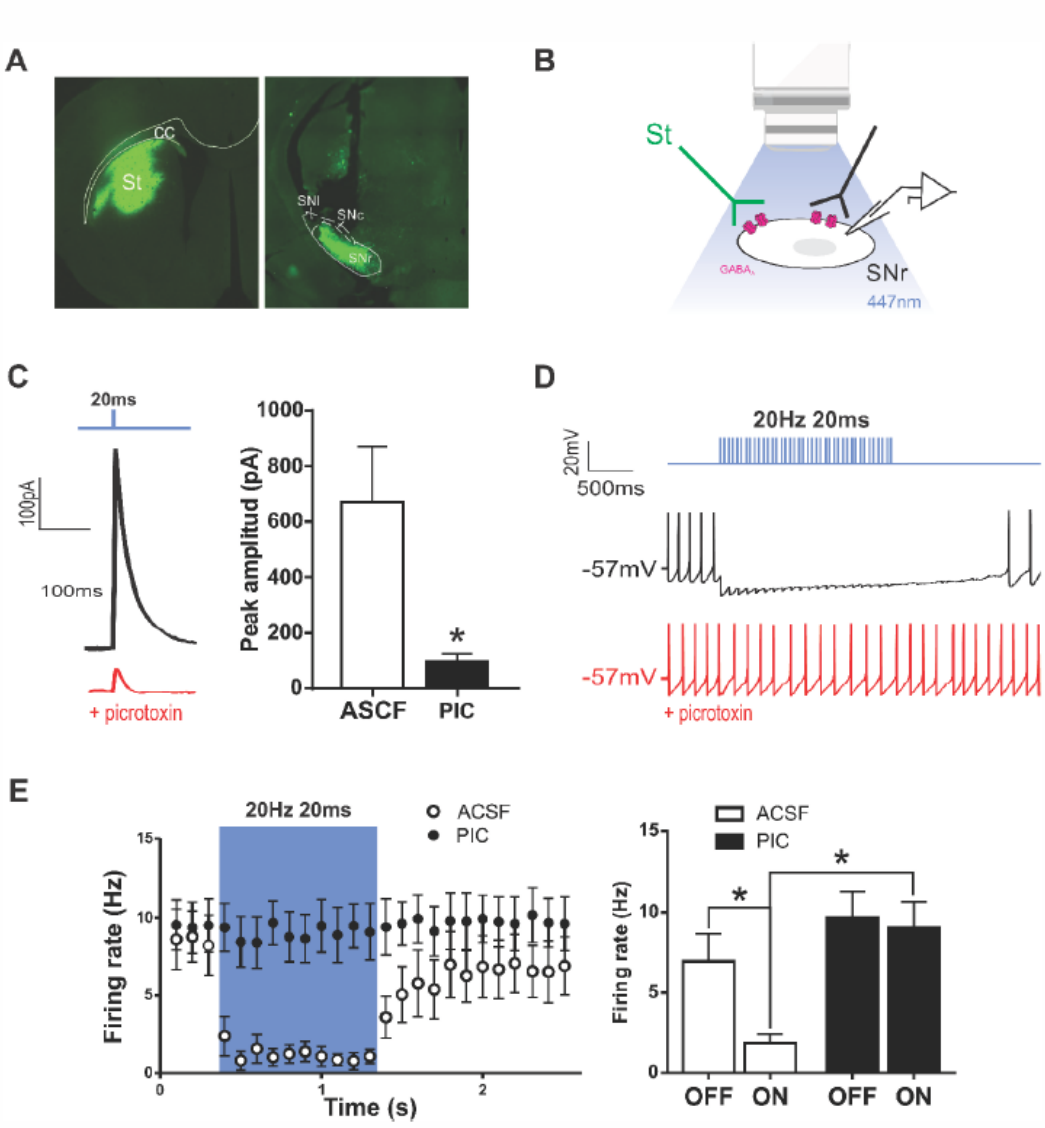

figure 1

Figure 1. Illumination of ChR2-transfected striatonigral terminals inhibits SNr neurons. A. Coronal sections of dorsal striatum (left) and the SNr (right) showing a representative injection site and ChR2-eYFP expression at striatonigral terminals, respectively. Note the track left by the fibre optic cannula in the SNr section. **B.** Schematic of the approach to ex vivo whole cell recording and illumination. **C.** Representative trace of an IPSC recorded at a holding potential of 0 mV in a SNr neuron, evoked by a 20 ms light pulse, before and after adding picrotoxin (50 uM) to the bath (left), and population data corresponding to ten SNr neurons recorded from five animals (right, * $p<0.05$, paired t test).

D. Representative current clamp recording of a SNr neuron inhibited during light stimulation of striatonigral terminals. **E.** Effect of trains of light pulses (20 ms, 20 Hz, ~8 mW) on the tonic firing of SNr neurons, before and after adding picrotoxin (50 uM) to the bath. Left: time course of effects. Bin size: 100 ms. Right: Data were integrated along the laser off and laser on periods and subjected to statistical analysis. 7 cells from 5 animals. *$p<0.05$, Bonferroni posthoc test after significant two way ANOVA interaction. Data are mean ± SEM. cc: corpus callosum; SNl: substantia nigra pars lateralis; SNc: substantia nigra pars compacta; SNr: substantia nigra pars reticulata; St: striatum

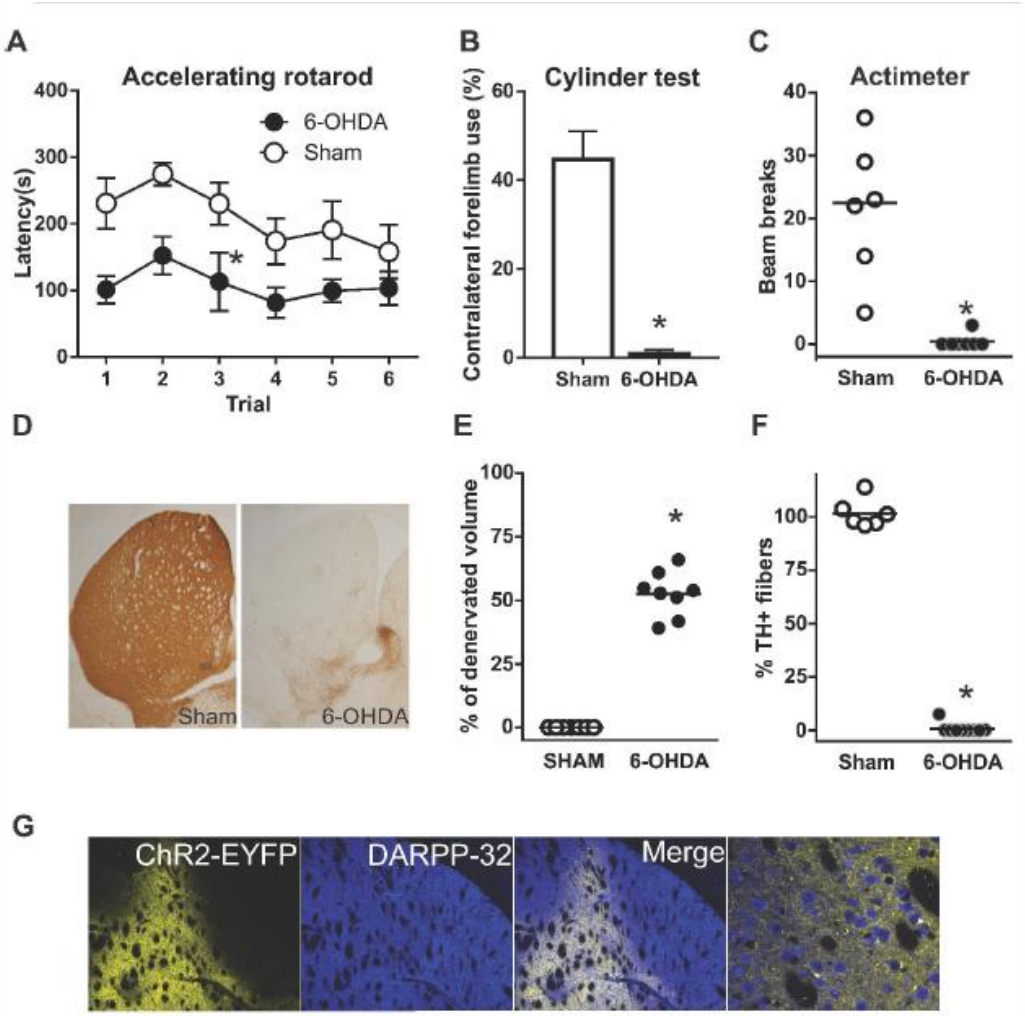

figure 2

Figure 2. Efficacy of dopamine lesions and channelrhodopsin viral infection. A-C. 6-OHDA-lesioned animals showed motor coordination deficits (**A;** * $p<0.05$, main effect of treatment, two way repeated measures ANOVA), reduced contralateral forelimb use (**B;** t-test, * $p<0.05$) and reduced vertical activity (**C;** Mann-Whitney test * $p<0.05$). D. Representative photomicrographs of striatal sections illustrating the loss of TH-positive fibres in 6-OHDA lesioned mice. **E-F.** The efficacy of 6-OHDA lesions was assessed by

quantifying the percentage of striatal volume that was completely denervated (**E**; Mann-Whitney test, * $p<0.05$) and striatal TH-positive fibre depletion (**F;** Mann-Whitney test * $p<0.05$). **G**. Representative low-magnification confocal images obtained from the striatum and SNr illustrating ChR2-EYFP expression in DARPP-32 neurons (striatum) and fibres (SNr) in AAV-ChR2 infected mice. Right-most panels show magnifications of the merge panels. Scale bars: 500μm, 50 μm. STR: striatum; SNr: substantia nigra reticulata., Sham n= 6; 6-OHDA n=8. Data are mean ± SEM for A and B, median and individual data points for C, E and F.

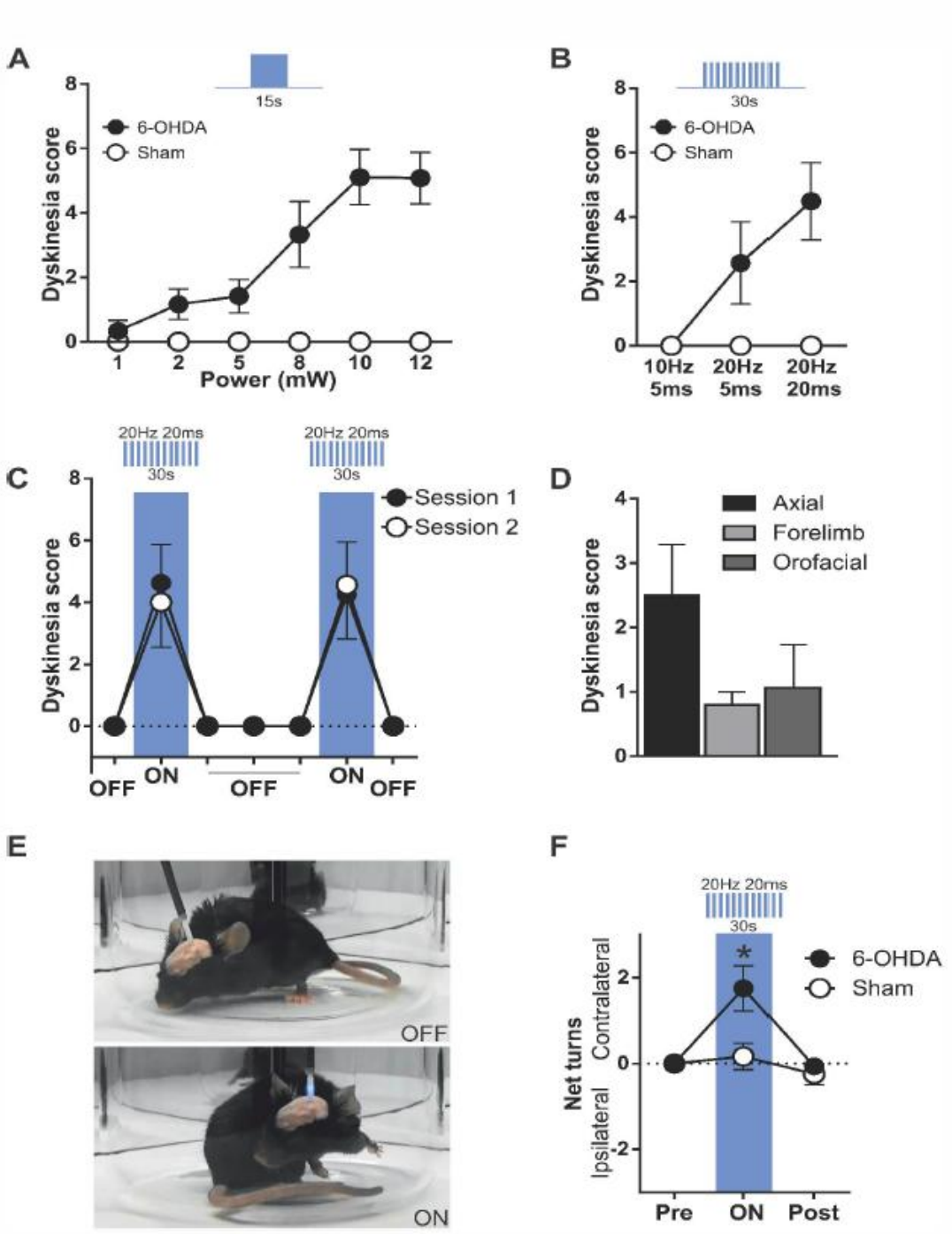

figure 3

Figure 3. Optostimulation of striatonigral terminals induces dyskinesia in 6-OHDA mice. Total dyskinesia (axial+forelimb+orofacial) score after continuous (**A**) or pulsatile (**B**) illumination of striatonigral terminals in 6-OHDA-lesioned mice. Note that illumination in sham-lesioned mice does not induce dyskinesia. **C.** Total dyskinesia score during striatonigral terminal stimulation showed inter-session and intra-session stability, two way repeated

measures ANOVA, inter-session main effect not significant, intra-session main effect not significant and interaction not significant. **D.** Types of dyskinesia observed during SNr illumination in 6-OHDA-lesioned mice. **E.** Photographs of 6-OHDA-lesioned mouse with laser OFF and laser ON. Optostimulation of striatonigral terminals induced dyskinesia. **F.** Rotational locomotive behaviour induced by the 20 Hz-20 ms protocol of optostimulation of striatonigral axon terminals in sham- and 6-OHDA-lesioned mice. * $p<0.05$, Bonferroni post hoc after two-way repeated measures ANOVA with significant interaction. Data are mean ± SEM. Sham n=6, 6-OHDA n=8.

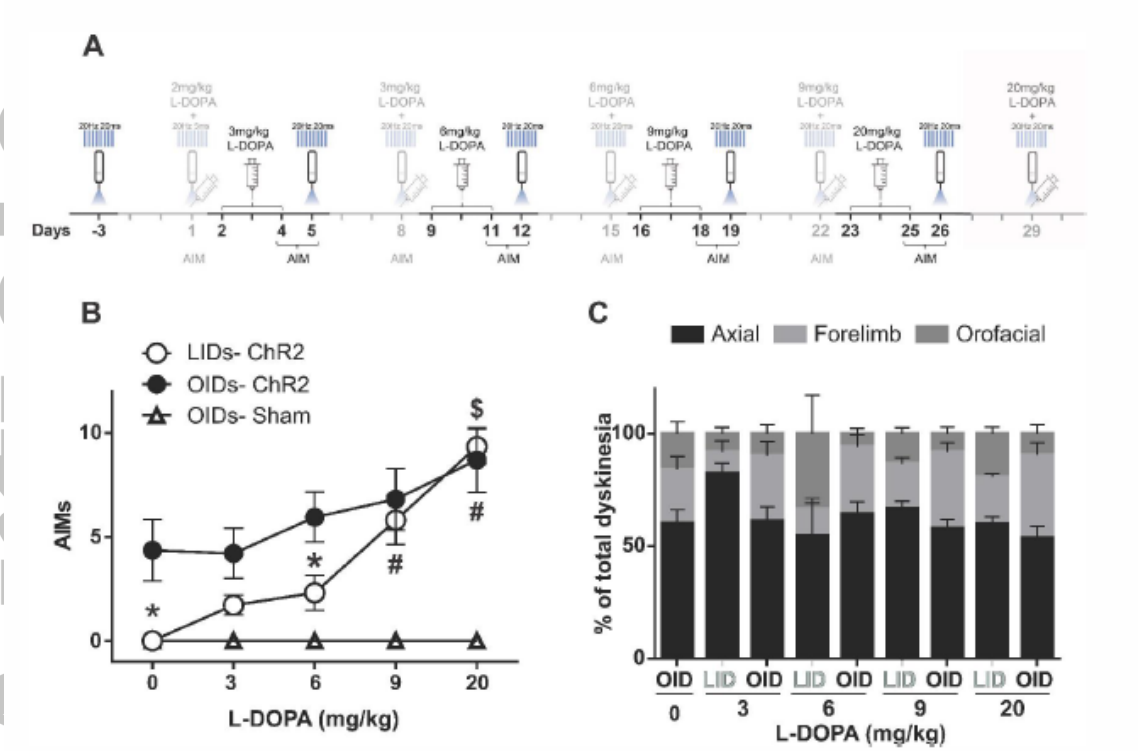

figure 4

Figure 4. Optostimulation of striatonigral terminals induces greater dyskinesia in primed than in naïve 6-OHDA mice. A. Experimental timeline highlighting in black the behavioural manipulation rated in B-C. **B.** Total dyskinesia score induced by 3 consecutive daily doses of L-DOPA (LID) or by optostimulation (OID) 24 h after the third day of each escalating dose of L-DOPA treatment. *p<0.05 OID vs LID; $ p<0.05 OID at 20 mg/kg vs OID at naïve and OID after 3 mg/kg L-DOPA; # p<0.05 LID at 9 or 20 mg/kg vs LID at 3 and 6 mg/kg L-DOPA; Bonferroni post hoc comparisons after significant interaction in a repeated measures two-way ANOVA. **C.** Type and intensity of dyskinesia induced by three days of each escalating dose of L-DOPA (LID) or by optostimulation (OID) applied 24 h after each third day of L-DOPA treatment. Data are mean ± SEM. Sham n=6, 6-OHDA n=8.

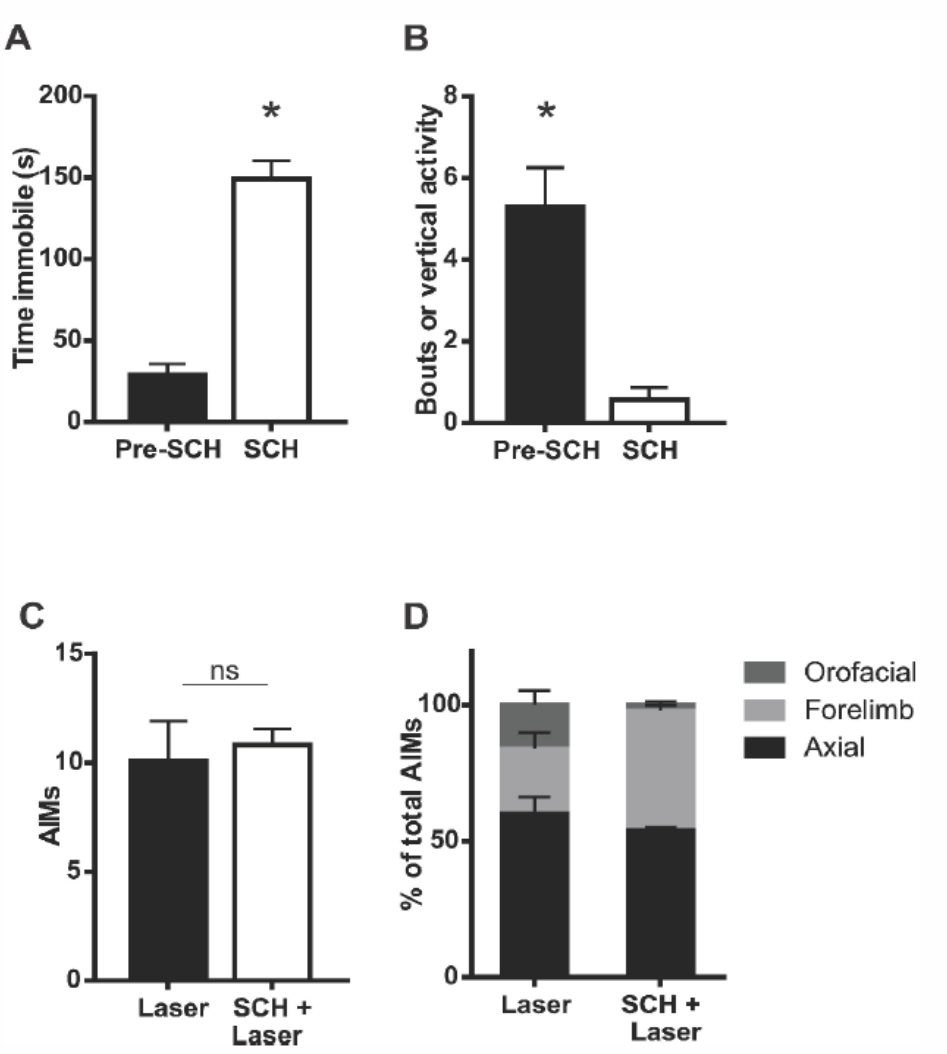

figure 5

Figure 5: The D1-type dopamine receptor antagonist SCH23390 does not modify optostimulation-induced dyskinesia. A and B. SCH23390 (0.25 mg/kg, i.p.) increases immobility (A; * $p<0.05$, paired t test) and reduces vertical activity (B; * $p<0.05$, paired t test) in 6-OHDA-lesioned mice. **C.** Total dyskinesia score (axial, orofacial, limb) induced by optostimulation of striatonigral terminals in 6-OHDA-lesioned mice, before and after administration of the D1-type receptor antagonist SCH23390 (0.25 mg/kg, i.p.). No significant difference was found (paired t test not significant) **D.** Composition of OID before and under the effect of SCH23390. Data are mean ± SEM, n=8 6-OHDA-lesioned mice.

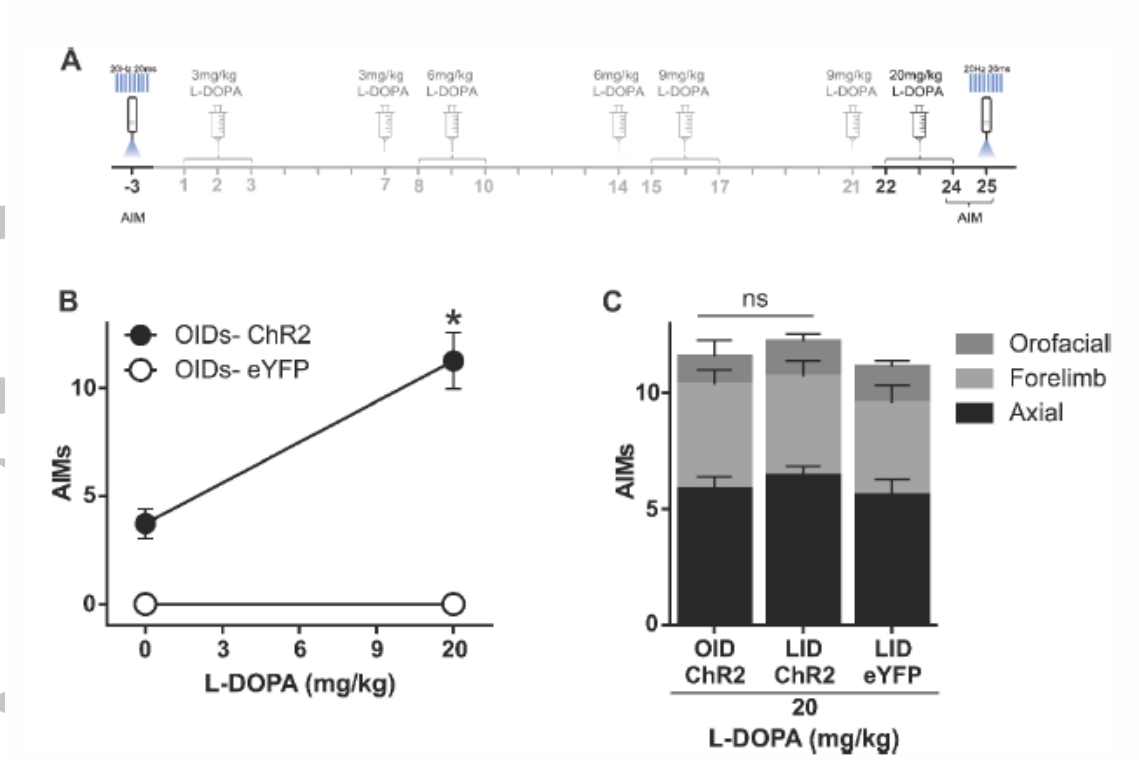

figure 6

Figure 6. Optostimulation in an independent set of animals confirms the L-DOPA priming effect on OIDs A. Experimental timeline highlighting in black the behavioural manipulation rated in B-C. **B.** OID observed in 6-OHDA-lesioned animals expressing ChR2-eYFP in striatonigral terminals (n=7) before and after chronic L-DOPA treatment (*p<0.05, paired t-test), and in an additional group of 6-OHDA-lesioned mice expressing eYFP only (n=7). **C.** Composition of total dyskinesia scores for OID after the chronic L-DOPA treatment shown in A, and for LID induced by 20 mg/kg L-DOPA in the same animals. Total AIM scores did not significantly differ between these conditions (paired t test not significant). Data are mean ± SEM

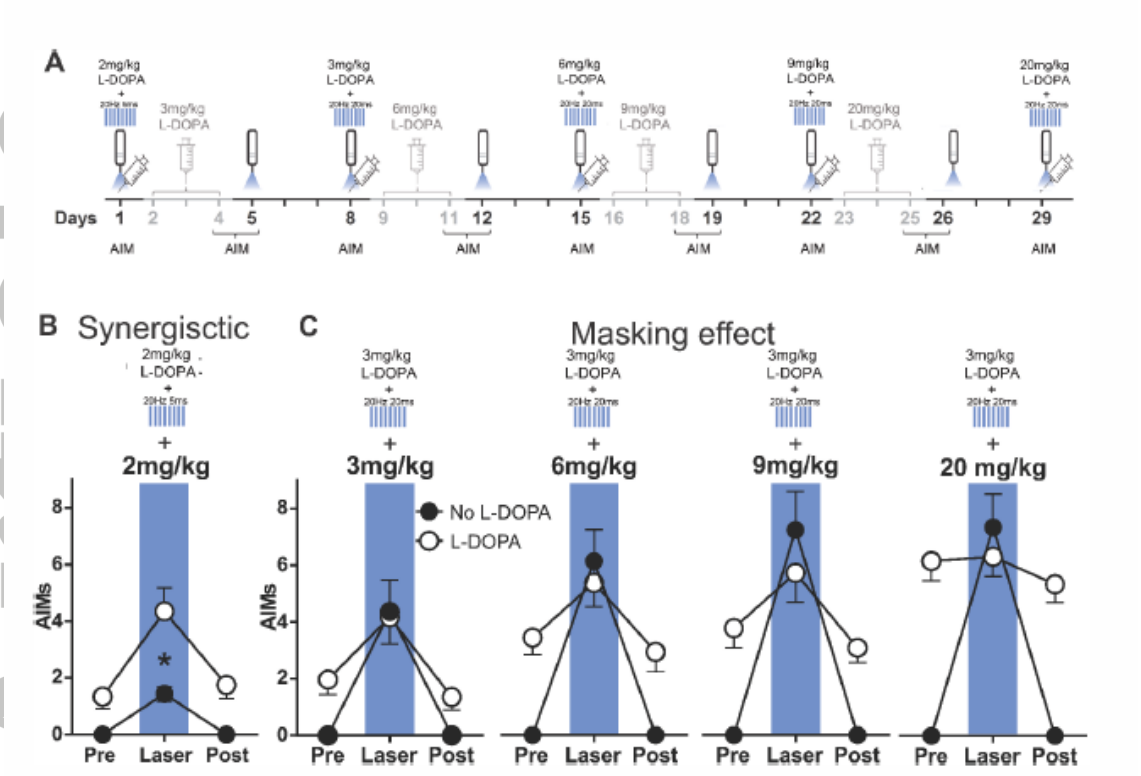

figure 7

Figure 7. Optical stimulation potentiates the effect of L-DOPA on dyskinesia. A. Experimental timeline highlighting in black the behavioural manipulations rated in B and C. **B.** Interaction between subthreshold illumination of striatonigral terminals (20 Hz-5 ms, 10 mW) and a low dose of L-DOPA (2 mg/kg) (n=14); * $p<0.05$, Bonferroni post hoc comparison after significant interaction in repeated measures two-way ANOVA. **C.** Interaction between suprathreshold illumination of striatonigral terminals (20 Hz-20 ms, 10 mW) and increasing doses of L-DOPA (3 to 20 mg/kg). Two-way ANOVA interactions reached significance at 3 (n=8), 6 (n=8), 9 (n=8) and 20 (n=12) mg/kg L-DOPA. Light stimulation plus L-DOPA did not differ from light stimulation alone at any of the conditions tested (Bonferroni posthoc comparisons). Data are mean ± SEM.

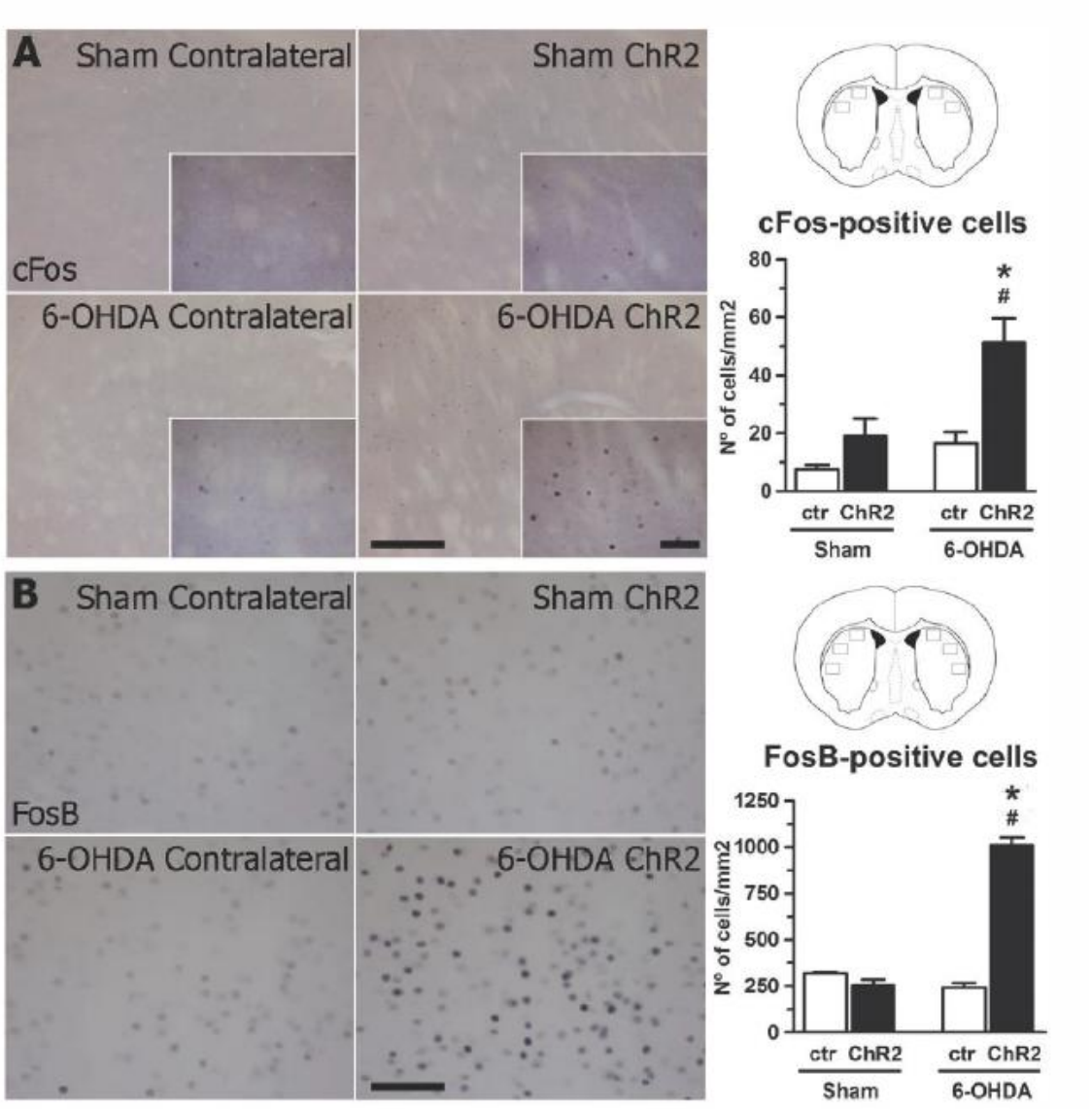

figure 8

Figure 8. Optostimulation of striatonigral axon terminals in the SNr induced subtle cFos expression in the striatum in 6-OHDA-lesioned animals. A. Left. High-power photomicrographs of sham- and 6-OHDA-lesioned mice, representing contralateral and ipsilateral (ChR2) striata immunostaining for cFos. **Right.** Locations of sampled areas are indicated by black boxes in the modified section from the Paxinos and Franklin (2001) brain atlas at 0.65 mm anterior to bregma. Histograms represent the quantification of cFos-immunoreactive nuclei. Note the higher expression in the ipsilateral striatum of 6-OHDA-lesioned mice. **B. Left.** High-power photomicrographs of sham- and 6-OHDA-lesioned mice

showing contralateral and ChR2 striatal immunostaining for FosB. **Right.** Sample locations as seen in A. Histograms represent FosB quantification. Also note the higher expression in ChR2 striatum. Data (mean ± SEM) were analysed by two-way ANOVA followed by posthoc test after significant interactions. * $p<0.05$ vs. sham ChR2; # $p<0.05$ vs. 6-OHDA contralateral. Scale bars: 200 µm and 50 µm.

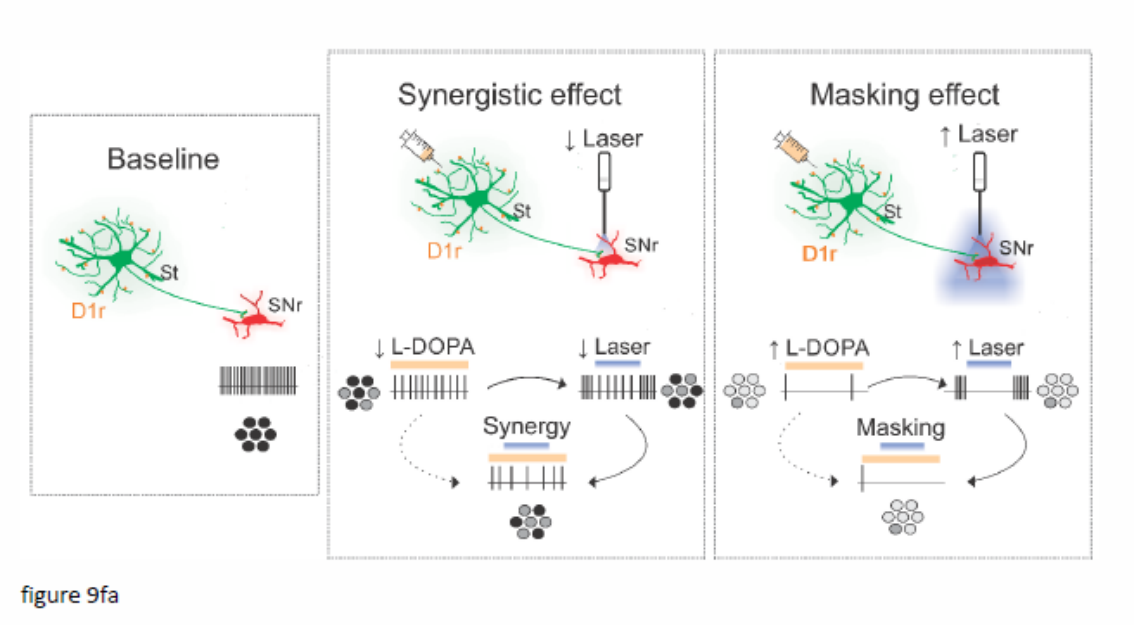

figure 9fa

Figure 9. Proposed mechanisms of the interacting effects of optostimulation and L-DOPA. Without stimulation, the SNr neurons fire action potentials tonically ("baseline"). When L-DOPA and light are delivered at low doses, their effects add to each other ("synergistic effect"). This could be explained by actions of both treatments on the same pathway (as illustrated) or on parallel pathways converging onto SNr neurons. In contrast, suprathreshold light stimulation masked the effect of even high doses of L-DOPA ("masking effect"), suggesting that stimulation of striatonigral axon terminals "clamps" basal ganglia output making it insensitive to actions of L-DOPA on the same or additional pathways. Circles in grayscale give out a population perspective of SNr neuronal activity.